A new approach to improve steady state and transient responses of AFPM motor regarding demagnetization phenomenon

N. Bahador, A. Darabi

Faculty of Electrical& Robotic Engineering, Shahrood University of Technology, Shahrood, Iran

Abstract. *In the ac machines, demagnetization phenomenon depending on its intensity changes the overall performance of machine via altering the waveform and amplitude of the Back EMF. By the way, due to existing complexity in the modeling of demagnetization, it has been considered hard to be taken into account precisely by the common design algorithm of machine. Therefore this paper proposes a modified approach for modeling and designing of ac PM machines specifically an axial flux permanent magnet motor in which the demagnetization is intended to be considered properly. In other word this technique improves steady state response of machine. Simulation results show the capability of presented modeling technique in compare with problematical classic and common designing and modeling approaches. Moreover this paper illustrates the benefit of applying a damper cage as a method of improving transient response of motor in demagnetizing situation if for any reasons, armature currents reduction would be impossible in transient operation regimes.*

Key words*: Axial Flux Permanent Magnet Motor, Modeling, Demagnetization, Damper Cage, 3D Finite Elements.*

I. INTRODUCTION

The permanent magnet materials which used for excitation in electrical drives have a great influence on PM machines. Changes in the magnetic properties of these PM materials can affect the performance characteristics of permanent magnet motors. These changes are basically classified into reversible and irreversible effects which both of them can be occurred by the reverse magnetic fields produced by armature coils. The effect of the armature mmf on the resultant field distribution is called armature reaction where depends on nature of load. The inverse magnetic flux produced by armature coils opposes the permanent magnet flux. This phenomenon changes the magnet's field and causes demagnetization of all or part of PM [1,2].

The subject of demagnetization phenomenon of permanent magnet machines have been investigated by several research groups [3,4,5,6,7,8]. They illustrated that the performance of PM machine would be degraded due to demagnetization [9,10,11]. It affects the design parameters of machines such as Back EMF. However, despite many undesirable effects, demagnetization phenomenon is not taken into account precisely by the common design algorithm of machine. This paper presents a modified approach for designing and modeling of permanent magnet machines. The proposed method considers the effects of demagnetization properly. The suggested algorithm is implemented for modeling of an axial flux permanent magnet motor.

Damping of magnetization variation in permanent magnet is also one of the other issues in modeling of electrical PM machines [11,12,13,14]. For this purpose, an anti-demagnetization method is proposed in this paper to protect PMs from transients. The studied solution is to use a appropriate damper cage in order to reduce the irreversible demagnetization rate down to acceptable levels.

Dampers are used in electric machines for various purposes, such as improving motor performance affected by transients. Damper designing has been the subject of many publications. Some authors have studied the influence of damper on the demagnetization of PM machines. For example, Hosoi et al. [13] showed that a damping cage can prevent demagnetization in the permanent magnet assisted salient pole synchronous machines. But there have not been any publications in using dampers to reduce demagnetization phenomenon in AFPM machines. This paper presentes a method for reducing irreversible demagnetization phenomenon during abrupt stopping of AFPM motor. Studied method is improving rotor structure by means of

applying a damper cage regarding the demagnetization during fast stopping. This paper focuses on the design of structure with damper cages and their capability in minimizing demagnetization.

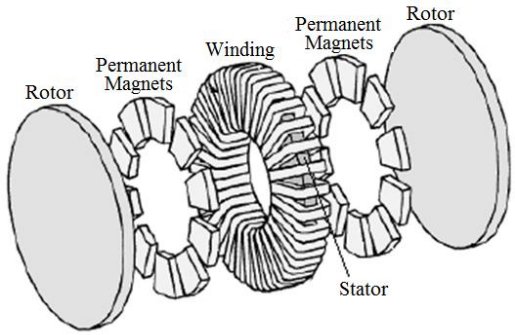

Fig. 1. Components of an Axial Flux Permanent Magnet motor

Table 1
Motor specification

Item	Value	Unit
Number of poles	*22*	
efficiency	*0.95*	
Nominal Power	*0.5*	*Mw*
Rotation Speed	*300*	*rpm*
frequency	*55*	*Hz*

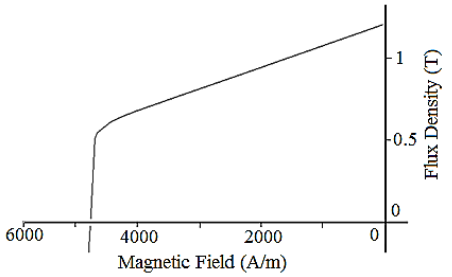

Fig. 2. Demagnetization curve of NEOMAX-42

II. MOTOR STRUCTURE OF CASE STUDY

Flat shape geometry and high torque capability make axial flux permanent magnet motors (AFPM motors) a preferred choice for industrial applications. Double-sided (TORUS) AFPM are the most widely used types. Topologies for Torus AFPM machines are “one stator two rotors” and “two stator one rotor”, which the first one has high torque to volume ratio [15,16]. Therefore, the design of a non-slotted, disc-type, TORUS AFPM motor is considered in this study. This motor is multi-layer kind one which one of its layers is studied here. The structure of motor is shown in figure 1. Machine's rated values are specified in Table 1. The rotor structure is designed by surface mounted NdFeB magnet which its demagnetization characteristic has been shown in figure 2 [17].

III. CLASSICAL DESIGN PROCEDURE OF AXIAL FLUX PERMANENT MAGNET MOTOR

For all the PM machines, design procedure is started by determining motor parameters through the classic design algorithm.

A. Classical design procedure

The main steps in classic design process are given as follows. First, machine's rated values such as output power, frequency, rated speed, terminal voltage and other parameters are typically specified for a special application. After that, the constant value for residual flux density of permanent magnets is determined by the designer at the begining of the design process. Then parameters such as magnetic and electric loadings are selected based on material saturation, cooper losses and temperature limitation. The machine dimensions, air gap diameter and machine stack length, are calculated based on output power, speed, etc. The internal and external stator and rotor diameter are also calculated. Another important design parameter to select is the value of current density for the stator windings. The self and mutual inductance of machines are calculated by means of FEM in the open circuit operating regime. Finally, the dynamic model of machine is obtained [17, 18]. The equation of classical design algorithm is summarized by the algorithm as follow:

1) Rated power

$$P_R \ [W]$$

2) Number of phases

$$m$$

3) Voltage rms value of phases

$$V_{ph} \ [V]$$

4) Rated frequency

$$f \ [Hz]$$

5) Rated speed

$$n \ [RPM]$$

6) Motor connection

$$\Delta \quad \text{or} \quad Y$$

7) Number of pole pairs

$$p = 60 f / n$$

8) Electric loading

$$\mathrm{A} \left[\frac{A}{m}\right] \quad 12000 \prec \mathrm{A} \prec 60000$$

9) Current density

$$\mathrm{J_s} \left[\frac{A}{m^2}\right] \quad 3(10^6) \prec \mathrm{J_s} \prec 10(10^6)$$

10) Number of parallel paths

$$a_p$$

11) Air gap flux density

$$B_g \quad [T]$$

12) The ratio of internal diameter vs. the outer diameter of machine

$$\lambda = \frac{D_i}{D_o}$$

13) Electrical power waveform factor

$$K_p$$

14) Current waveform factor

$$K_i$$

15) Electro motive force factor

$$K_e = \pi K_w$$

16) Slot fill factor

$$K_{cu}$$

17) The ratio of stator pole arc portion to the stator pole pitch portion

$$\alpha_i \quad (0.7 \prec \alpha_i \prec 0.9)$$

18) Recoil relative permeability of permanent magnet

$$\mu_{rPM}$$

19) Residual flux density of permanent magnet

$$B_r \quad [T]$$

20) Flux density in rotor core

$$B_{cr} \quad [T]$$

21) Flux leakage factor

$$K_d = (1 - p/30)$$

22) Attainable flux density

$$B_u = B_g / K_d \quad [T]$$

23) Machine efficiency

$$\eta$$

24) Diameter of outer surface of machine

$$D_o = \left(\frac{4 p P_R}{N_{stator}\ \pi\ K_e\ K_i\ K_p \eta\ B_g A\ f (1-\lambda^2)(1+\lambda)}\right)^{\frac{1}{3}} \quad [m]$$

25) Internal diameter of machine

$$D_i = \lambda D_o \quad [m]$$

26) Average diameter of airgap

$$D_g = \frac{D_o + D_i}{2} = \frac{1+\lambda}{2} D_o \quad [m]$$

27) Axial length of airgap

$$g \quad [m]$$

28) Flux density in stator core

$$B_{cs} = 5.47 f^{-0.32} \quad [T]$$

29) Protrusion of end winding

$$W_{cuo} = \frac{\sqrt{D_o^2 + \frac{4 A_s D_g}{K_{cu} J_s}} - D_o}{2} \quad [m]$$

30) Axial length of stator

$$L_s = L_{cs} + 1.6 W_{cui} \quad [m]$$

31) Axial length of rotor disk

$$L_{cr} = \frac{B_u\ \pi\ D_o (1+\lambda)}{B_{cr} 8 p} \quad [m]$$

32) PM length

$$L_{PM} = \frac{\mu_{rPM}\ B_g}{B_r - \frac{K_f}{K_d} B_g} (g + W_{cu}) \quad [m]$$

33) Axial length of rotor

$$L_r = L_{cr} + L_{PM} \quad [m]$$

34) Effective stack length of machine

$$L_e = L_s + 2 L_r + 2 g \quad [m]$$

35) The peak value of the phase airgap EMF

$$E_{PK} = K_V V_{ph} \quad [V]$$

36) Number of turn per phase

$$N_t = \frac{E_{PK}}{K_e\, B_g\, \frac{f}{p}(1-\lambda^2)\, D_o^2}$$

37) RMS value of Winding current

$$I_{rms} = \frac{\pi\, D_g A_s}{2 m_1 N_t} \quad [A]$$

38) Surface area of stator conductor

$$s_a = \frac{I_{rms}}{J_s} \quad [cm^2]$$

B. Designed AFPM motor

The initial designing of TORUS-NS machine was performed using classical algorithm. The machine required to be operated in leading power factor just because we were sure that the actual value for back-EMF will be less than the expected value, due to the chosen magnet material and the occurrence probability of the demagnetization. In order to achieve this goal, the larger value is assumed for back-EMF constant. The designing results for AFPM motor are tabulated in Table 2. The speed, torque and efficiency of the motor are also presented in figure 3 and 4.

Table 2
Design Parameters and Dimensions

Property	Units	Value
Number of Pole Pairs		*11*
Magnetic Loading	*T*	*0.6974*
Electric Loading	*A/m*	*60000*
Total Loss	*25*	*kW*
Copper Loss	*9.5*	*kW*
Current Density	*A/mm²*	*10*
Residual Flux Density of The PM Material	*T*	*1.2*
Flux Density in The Stator Core	*T*	*1.5173*
Air Gap Length	*m*	*0.005*
External Diameter	*m*	*1.2953*
Internal Diameter	*m*	*0.7473*

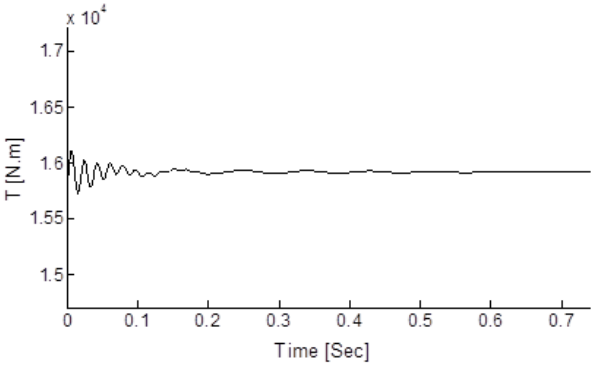

Fig. 3. Instantaneous torque

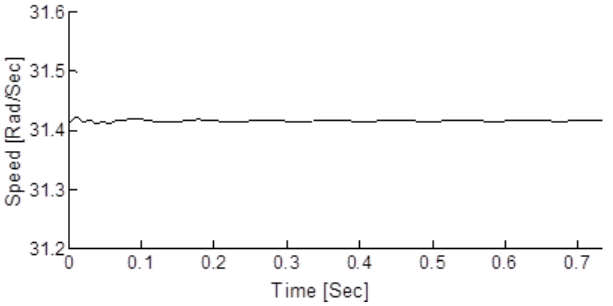

Fig. 4. Rotor mechanical speed

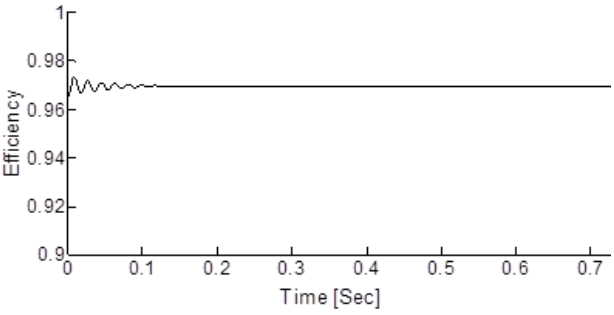

Fig. 5. Motor Efficiency

IV. MODELING OF DESIGNED AFPM MOTOR

After the initial designing has been completed, AFPM motor needs to be modeled.The finite element method is used to extract equivalent circuit parameters of machine.

This machine is three-phase, multiple layers motor. Only one layer of multi-layers AFPM motor is modeled, because of independent geometry of each layer and no magnetic coupling between them.

It is also seen that the motor effectively comprises two independent halves, lying either side of the radial centerline. Because of symmetry condition only half part of motor is simulated.

The Axial flux motor possesses a complex

magnetic circuit and requires three dimensional FEA models due to its three dimensional (3D) magnetic circuits. One pole pair of motor is shown in figure 6.

The motor electromagnetic parameters are obtained by means of FEM analyses. The flux density and magnetic field strength distribution over the model is obtained. The self and mutual inductance of machines and flux linkages are calculated by means of FEM in the open circuit operating regime. Finally, the dynamic model of machine is extracted.

Then the dynamic model of motor is simulated in Matlab software and the operation characteristics of machine are extracted.

According to the results, the rms value of induced voltage became 1.3396 per unit. The results also showed that the motor operate in 0.84 leading power factor at full load condition.

Figure 7 shows the air-gap flux density over one pole using FEA. But this modeling approach gives wrong design results just because the demagnetization phenomenon was not considered through the machines design and modeling procedure.

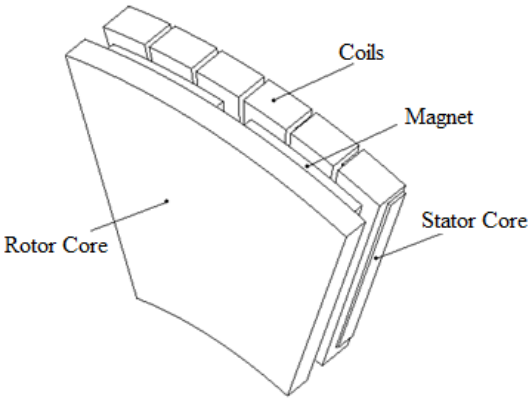

Fig. 6. One pole pair of motor

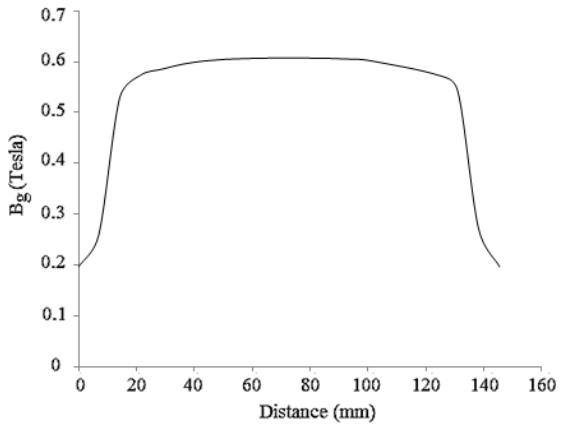

Fig. 7. Open circuit air-gap flux density of the AFPM motor

V. ARMATURE REACTION AND DEMAGNETIZATION

The second quadrant of the hysteresis curve of the magnetic material referred to as the demagnetization curve. Each of the demagnetization curves has a bend in it, mentioned as the "knee". The irreversible demagnetization of a permanent magnet occurs when the operating points take place below the linear section of the B-H curve and then the magnet cannot recover its original magnetization even when brought back to the initial condition. After removing the demagnetization factor, the operating point will move along the recoil curve. The recoil curve is in parallel with the tangential line to the B-H curve at H=0 and B= B_r (figure 8). The rate of permanent magnets demagnetization is obtained based on the difference between the present estimated residual flux density and the reference value (residual flux density value having been obtained in a normal state).

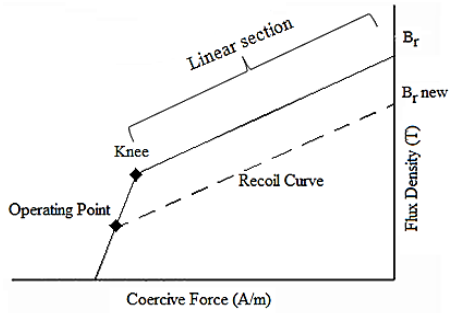

Fig. 8. Demagnetization curve

The Percentage of residual flux density reduction indicates the demagnetization ratio, as in (a).

Demagnetization Ratio= $(1-\frac{B_{r\,new}}{B_{r\,initial}}) \times 100$ (a)

$B_{r\,new} = B'_r \times$ (Percentage of Average Demagnetized Area)+ $B_{r\,initial} \times$ (1- Percentage of Average Demagnetized Area)

$B_{r\,initial}$: Permanent Magnet Residual Flux Density before Demagnetization

B'_r : Average Residual Flux Density of Demagnetized Area

$B_{r\,new}$: Permanent Magnet Residual Flux Density after Demagnetization

When the machine operates *at* no load condition, zero armature current, the operating point of magnet *does* not change much and demagnetization will not take place. But when the machine operates under load and the magnet is subjected to the armature reaction, the operating point may move and may not come back to the original operating point. Therefore at different loading conditions, the waveform of Back EMF, sinusoidal or trapezoidal, may change. The change rate of Back EMF depends on reduction rate of air gap flux density and consequently the level of armature reaction mmf.

Since the residual magnetism of permanent magnets changes under different loading conditions due to the armature reaction fields, the residual flux density may not remain constant. Thus the value of the Back EMF also changes. Therefore, this modeling approach gives wrong design results.

VI. COMPARISON BETWEEN MACHINE MODELING WITH AND WITHOUT CONSIDERING DEMAGNETIZATION

As described above, the primary design of AFPM motor was done using classical algorithm and accordingly the characteristics of machine are extracted.

By implementing the iterative algorithm between finite element and dynamic model, the rms value of back-EMF becomes fixed after four iterations. Table 3 lists the values of induced voltage and demagnetization ratio at each iteration.

Table 3
Comparison between machine modeling with and without considering demagnetization

Iteration	Demagnetization rate (%)	RMS value of back-EMF (pu)
Primary step in design	*0*	*1.3396*
1	*11*	*1.2863*
2	*19.166*	*1.205*
3	*20*	*1.1638*
4	*20*	*1.1638*

In AFPM motors, the air gap flux density is one of the significant design parameter. A small change of it has important influence on the motor characteristics. At each iteration, magnetic flux density distribution over one pole is shown in figure 9. As shown, the PM demagnetization degrades the air gap flux density and consequently the resultant back EMF waveform. It leads to a non-trapezoidal air gap flux density.

This motor is designed to operate in 0.84 leading power factor using classical algorithm, but as shown in Table 4, the severe demagnetization causes this motor to operate at nearly unity power factor mode.

Table 4
Rated power factor

Iteration	*Demagnetization rate (%)*	*Rated power factor*
Primary design step	0	0.84 leading
4	20	0.9977 leading

The results showed that the values of motor performance parameters do not fall within the expected range. So we can see the lack of consideration of this phenomenon may entail unanticipated and unintended consequences.

Therefore, the initial motor structure must be modified in order to minimize demagnetization. One of the methods to reduce the demagnetizing effect is to setting up a damping system in rotor structure in order to avoid the direct effect of the armature demagnetizing field in transients. For this propose, damper cage are added to rotor structure without changing the stator specifications. The minimum weight of the damper case and being easily mounted to the rotor is also considered.

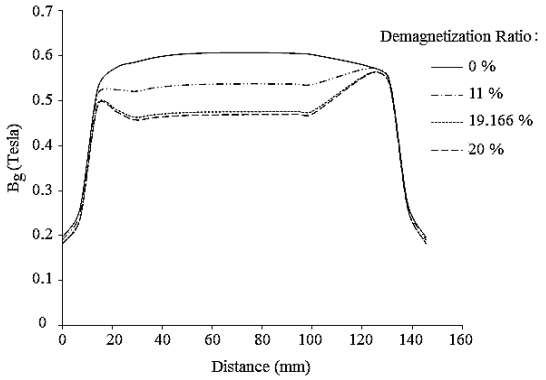

Fig.9. Full Load Air gap flux density at average diameter

VII. Using damper cage for reducing demagnetization

This section provides three different types of damper cages to reduce the demagnetization effects. The following results demonstrate the efficiency of dampers in minimizing demagnetization rate.

A. Studied condition

Some type of industrial applications requires that

a rotary mechanism be stopped quickly. In AFPM motors during emergency braking, the large instantaneous current passes through the armature winding which may causes demagnetization of PMs. In AFPM motor considered in this study, because of high inertia, it is sometimes difficult to abruptly stop. For AFPM motor, dynamic braking is easily achieved by disconnecting the machine from main supply and shorting the motor terminals, thus bringing the motor to a fast stop. In this mode of operation, a braking torque is created by the interaction of a constant magnetic flux in an electric motor with magnetic flux produced by the current of short-circuiting the armature winding. During abrupt stopping, the large instantaneous current, which passes through the armature winding, may causes demagnetization of PMs. Therefore, it is necessary to investigate the possibility of demagnetization occurrence.

Considering figure 10, as motor operates under full load condition, at time t_0, first terminals have been disconnected from main supply, then immediately afterwards (at time t_1) a three phase short circuit is occurred in stator winding. The short circuit currents waveform, are shown in figure 11.

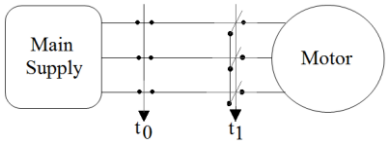

Fig. 10. Fast stopping process

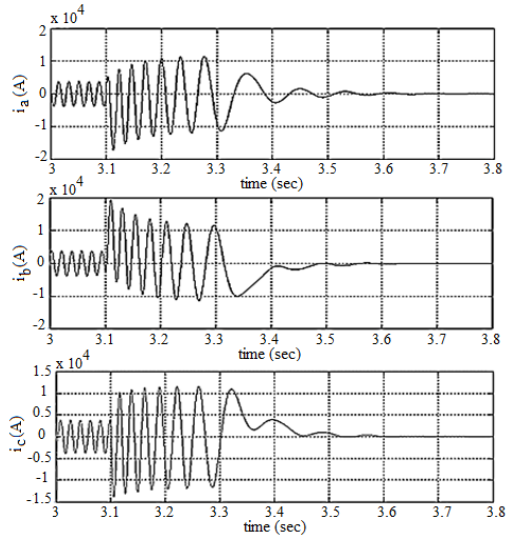

Fig. 11. Stator currents during fast stopping

B. Damper structure 1

In first structure, the copper bars housed in the slot in the middle of magnets. The damper bars are short circuited at the ends by short circuiting rings. Figure 12 shows a single pair of magnets with the proposed additional damper bars. The damper cage is being fixed to the rotor disc.

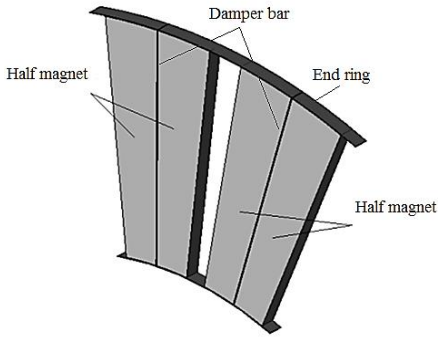

Fig. 12. Damper structure 1

When armature reaction flux lines cut damper bars, an eddy current will be induced in them that oppose the magnetic flux variation. This current should generate a magnetic field to keep the overall PM flux constant. Considering figure 13, this type of damper has little effect and is not able to strongly reduce demagnetization rate.

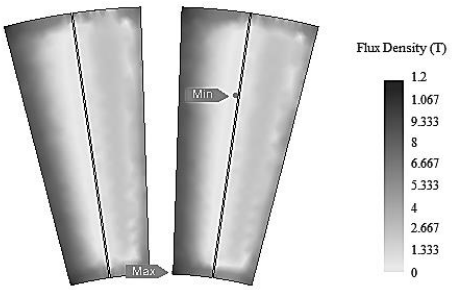

Fig. 13. Flux density contour plot of the magnet after adding damper 1

C. Damper structure 2

Figure 14 shows a different type of damper. Considering this structure, one copper bar housed in the slot in the middle of magnet and two bars are provided around the permanent magnet. The ends of damper bars of each magnet are short circuited. Considering figure 15, this kind of damper has also little effect on PM's flux variation.

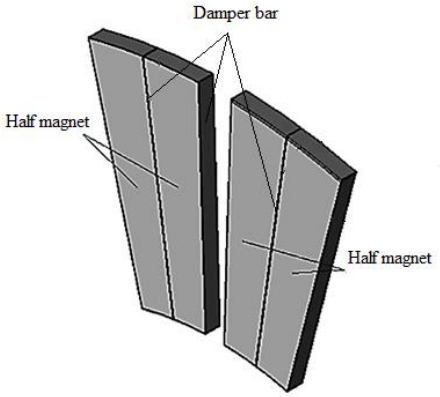

Fig. 14. Damper structure 2

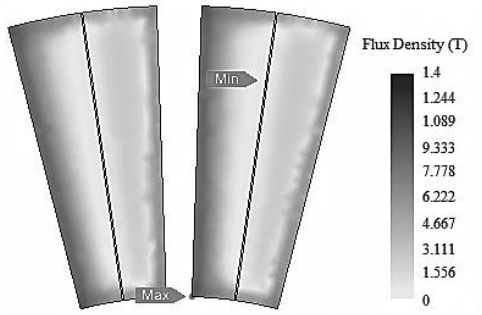

Fig. 15. Flux density contour plot of the magnet after adding damper 2

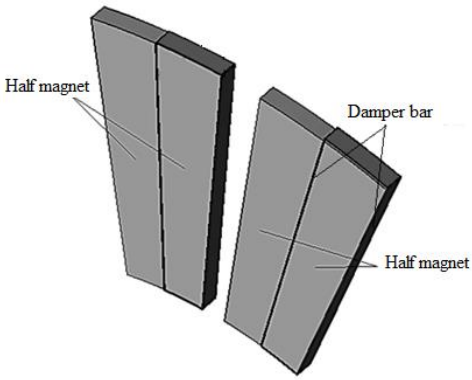

Fig. 16. Damper structure 3

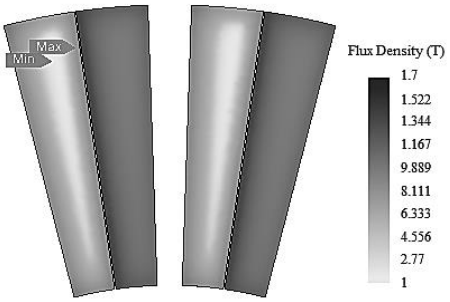

Fig. 17. Flux density contour plot of the magnet after adding damper 3

D. Damper structure 3

In third structure, as Figure 16 shows, a narrow conductive frame surrounds the demagnetized area in magnets. A current is induced in the frame when magnetic flux changes through the frame. The induced current's magnetic field opposes the change in the magnetic flux that induced the current.

However this method is used only for fixed direction of motor's rotation, but considering figure 17, the results of finite element analysis show that the proposed damper could effectively reduce demagnetization rate.

A comparison among these dampers is carried out and their damping performance to reduce irreversible demagnetization is presented in Table 5 and figure 18. The analysis results demonstrate that the third damper led to a larger damping effect and far fewer losses (about 4 percent of total stator copper loss) than the other two types of dampers. These low damper's losses would not have a considerable impact on Motor efficiency.

Table 5
Comparison among analysis results

Item	Average demagnetization area in each PM (%)	Average demagnetization ratio (%) (first iteration)
Without damper	*72.38*	*20*
Rotor design 1	*69.38*	*19.25*
Rotor design 2	*66.99*	*17.94*
Rotor design 3	*11.006*	*2.75*

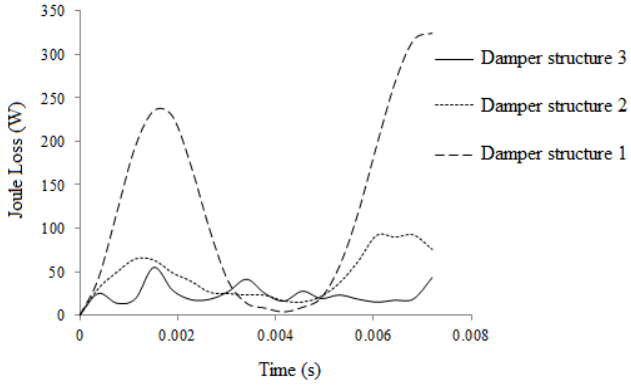

Fig. 18. Losses of one damper in 3 topologies

VIII. CONCLUSION

Since the permanent magnets in a PM machine play a significant rule, even a minor variation of their magnetic properties can reduce the machine performance considerably. Demagnetization is one of the phenomena that may cause a major change in the properties of magnets. This phenomenon, depending on its intensity, changes the machine performance characteristics via altering the amplitude and waveform of the Back EMF. However, despite of many undesirable effects, demagnetization phenomenon is not taken into account precisely in common design algorithm of machine.

This paper presented a modified approach for designing and modeling of the permanent magnet machines. The proposed method considered the effects of demagnetization properly. The suggested algorithm was implemented for modeling of an axial flux permanent magnet motor. Simulation results

presented in this report showed that the classic designing and modeling method may Give inaccurate results. Moreover this report illustrated the benefit of applying a damper cage regarding the demagnetizing if for any reasons, armature currents reduction be impossible in the transient operation regimes. Three different types of damper cages were provided to reduce the demagnetization effects. The results demonstrated the efficiency of third damper in minimizing demagnetization. The demagnetization rate decreased 86.25% compared to initial design. It should be noted, that the mentioned structure is used only for fixed direction of motor's rotation. As a result, in surface mounted permanent magnet motors with low reluctance path for the armature reaction field (because of the narrow gap between the magnets and stator disk), using damper cage in rotor structure is a good and simple way to prevent demagnetization.

REFERENCES

1. Ruoho S., Dlala E., Arkkio A. (2007). Comparison of Demagnetization Models for Finite-Element Analysis of Permanent-Magnet Synchronous Machines. *IEEE Trans. Magn.*, vol. 43, no. 11.
2. Ruoho S. (2011). Modeling Demagnetization of Sintered NdFeB Magnet Material in Time-Discretized Finite Element Analysis. *Aalto University School of Electrical Engineering. Espoo, Finland.*
3. Morimoto S., Takeda Y., Hirasa T., Taniguchi K. (1990). Expansion of Operating Limits for Permanent Magnet Motor by Current Vector Control Considering Inverter Capacity. *IEEE Transactions on Industry Applications*. vol. 26, No. 5, pp: 866-871.
4. Ooshima M., Miyazawa S., Chiba A., Nakamura F., Fukao T. (1997). A Rotor Design of a Permanent Magnet-Type Bearingless Motor Considering Demagnetization. *Power Conversion Conference, Nagaoka*. vol. 2, pp: 655-660.
5. Kang Do Hyun, Curiac P., Lee Ju (2000). An Axial Flux Interior PM Synchronous Machine. *In Proc. ICEM 2000, Espoo Finland.* pp: 1475-1479.
6. Arshad W. M., Chin Y. K., B.ckstr.m T., Soulard J., .stlund S., Sadarangani C. (2001). On Finding Compact motor Solutions for Transient Applications. *Electric Machines and Drives Conference, Cambridge, MA, USA.* pp: 743-747.
7. Goldenberg C., Lebensztajn L., Lobosco O.S. (1997). Analysis of short circuit transients of a PM machine. *Electric Machines and Drives Conference Record, Milwaukee, USA*. pp: WB2/13.1-WB2/13.3.
8. Rosu M., Arkkio A., Jokinen T., Mantere J., Westerlund J. (1999). Demagnetisation State Of Permanent Magnets In Large Output Power Permanent Magnet Synchronous Motor. *In Proc. International Conference IEMD '99, Seattle, USA*, pp: 776-778.
9. Kang G.-H., Hur J., Nam H, Hong J.-P., and Kim G.-T. (2003). Analysis of irreversible magnet demagnetization in line-start motors based on the finiteelement method. *IEEE Trans. Magn.*, vol. 39, no. 3, pp: 1488-1491.
10. Yang Y., Wu ch. (2010). Study of Anti-Demagnetization Property for a Flux-Shunt Permanent Magnet DC Motor. *IEEE International Conference on Industrial Technology (ICIT).* pp: 422 – 426.
11. Xing J., Wang F., Wang T., Zhang Y. (2010). Study on Anti-Demagnetization of Magnet for High Speed Permanent Magnet Machine. *IEEE TRANSACTIONS ON APPLIED SUPERCONDUCTIVITY*, VOL.20, NO. 3, pp: 856 – 860.
12. Hwang K., Yang B., Rhyu S., Kim B., Kim D., Rhee S., Kwon B. (2009). Optimal rotor design for reducing the partial demagnetization effect and cogging torque in spoke type PM motor. *JOURNAL OF APPLIED PHYSICS*.
13. Hosoi T., Watanabe H., Shima K., Fukami T., Hanaoka R., Takata S. (2010). Demagnetization Analysis of Additional Permanent Magnets in Salient-Pole Synchronous Machines under Sudden Short Circuits. *International Conference on Electrical Machines, Rome*.
14. Shin H., Kim T., Kim C. (2011). A Study on Irreversible Permanent Magnet Demagnetization in Flux-Reversal Machines. *International Conference on Electrical Machines and Systems*.
15. Mahmoudi A., Kahourzade S., Rahim N. A., and Ping W. P. (2012). Improvement to performance of solid-rotor-ringed line-start axial flux permanent-magnet motor. *Progress In Electromagnetics Research*, Vol. 124, p: 383-404.
16. Gerlando A. Di., Foglia G., and Perini R. (2008). Permanent magnet machines for modulated damping of seismic vibrations: Electrical and thermal modeling. *IEEE Trans. on Ind. Electron*. Vol. 55, No. 10, p: 3602-3610.
17. Darabi A., Moradi H., and Azarinfar H. (2012). Design and Simulation of Low Speed Axial Flux Permanent Magnet (AFPM) Machine. *Engineering and Technology 61*.
18. Huang S., Aydin M., Lipo T.A. (2001). TORUS concept machines: pre-prototyping design assessment for two major topologies. *Industry Applications Conference, Thirty-Sixth IAS Annual Meeting*. Volume 3, pp.:1619 -1625.